Sciencexpress Report

Discovery of Powerful Gamma-Ray Flares from the Crab Nebula

M. Tavani,[1,2,3,4] A. Bulgarelli,[5] V. Vittorini,[1] A. Pellizzoni,[16] E. Striani,[2,4] P. Caraveo,[7] M.C. Weisskopf,[21] A. Tennant,[21] G. Pucella,[6] A. Trois,[1] E. Costa,[1] Y. Evangelista,[1] C. Pittori,[19] F. Verrecchia,[19] E. Del Monte,[1] R. Campana,[1] M. Pilia,[16,17] A. De Luca,[7,25] I. Donnarumma,[1] D. Horns,[22] C. Ferrigno,[23] C.O. Heinke,[24] M. Trifoglio,[5] F. Gianotti,[5] S. Vercellone,[18] A. Argan,[1] G. Barbiellini,[3,8,9] P.W. Cattaneo,[10] A.W. Chen,[3,7] T. Contessi,[7] F. D'Ammando,[18] G. DeParis,[1] G. Di Cocco,[5] G. Di Persio,[1] M. Feroci,[1] A. Ferrari,[3,11] M. Galli,[12] A. Giuliani,[7] M. Giusti,[1,3] C. Labanti,[5] I. Lapshov,[13] F. Lazzarotto,[1] P. Lipari,[14,15] F. Longo,[8,9] F. Fuschino,[5] M. Marisaldi,[5] S. Mereghetti,[7] E. Morelli,[5] E. Moretti,[8,9] A. Morselli,[4] L. Pacciani,[1] F. Perotti,[7] G. Piano,[1,4] P. Picozza,[1,4] M. Prest,[17] M. Rapisarda,[6] A. Rappoldi,[10] A. Rubini,[1] S. Sabatini,[1,4] P. Soffitta,[1] E. Vallazza,[9] A. Zambra,[3,7] D. Zanello,[14,15] F. Lucarelli,[19] P. Santolamazza,[19] P. Giommi,[19] L. Salotti,[20] G.F. Bignami[25]

[1]INAF-IASF Roma, via del Fosso del Cavaliere 100, 00133 Roma, Italy. [2]Dipartimento di Fisica, Università degli Studi di Roma “Tor Vergata”, via della Ricerca Scientifica 1, 00133 Roma, Italy. [3]Consorzio Interuniversitario Fisica Spaziale (CIFS), villa Gualino, v.le Settimio Severo 63, 10133 Torino, Italy. [4]INFN Roma Tor Vergata, via della Ricerca Scientifica 1, 00133 Roma, Italy. [5]INAF-IASF Bologna, via Gobetti 101, 40129 Bologna, Italy. [6]ENEA Frascati, via Enrico Fermi 45, 00044 Frascati(RM), Italy. [7]INAF-IASF Milano, via E. Bassini 15, 20133 Milano, Italy. [8]Dip. Fisica, Università di Trieste, via A. Valerio 2, 34127 Trieste, Italy. [9]INFN Trieste, Padriciano 99, 34012 Trieste, Italy. [10]INFN Pavia, via Bassi 6, 27100 Pavia, Italy. [11]Dipartimento di Fisica Generale, Università degli Studi di Torino, via P. Giuria 1, 10125 Torino, Italy. [12]ENEA Bologna, via don Fiammelli 2, 40128 Bologna, Italy. [13]IKI, Moscow, Russia. [14]INFN Roma 1, p.le Aldo Moro 2, 00185 Roma, Italy. [15]Dipartimento di Fisica, Università degli Studi di Roma “La Sapienza”, p.le Aldo Moro 2, 00185 Roma, Italy. [16]INAF Osservatorio Astron. Cagliari, Poggio dei Pini, 09012 Capoterra, Italy. [17]Dipartimento di Fisica, Università degli Studi dell’ Insubria, via Valleggio 11, 22100, Como, Italy. [18]INAF IASF Palermo, via La Malfa 153, 90146 Palermo, Italy. [19]ASI Science Data Center, ESRIN, 00044 Frascati, Italy. [20]Agenzia Spaziale Italiana, viale Liegi 26, Roma, Italy. [21]NASA, Marshall Flight Space Center, Huntsville, Alabama USA. [22]Institut fuer Experimentalphysik, University of Hamburg, Germany. [23]ISDC, University of Geneva, Switzerland. [24]University of Alberta, Edmonton, AB T6G 2G7, Canada. [25]IUSS, Pavia, Italy.

The well known Crab Nebula is at the center of the SN1054 supernova remnant. It consists of a rotationally-powered pulsar interacting with a surrounding nebula through a relativistic particle wind. The emissions originating from the pulsar and nebula have been considered to be essentially stable. Here we report the detection of strong gamma-ray (100 MeV-10 GeV) flares observed by the AGILE satellite in September, 2010 and October, 2007. In both cases, the unpulsed flux increased by a factor of 3 compared to the non-flaring flux. The flare luminosity and short timescale favor an origin near the pulsar, and we discuss *Chandra* Observatory X-ray and *HST* optical follow-up observations of the nebula. Our observations challenge standard models of nebular emission and require power-law acceleration by shock-driven plasma wave turbulence within a ~1-day timescale.

The Crab Nebula (*1*) is a relic of a stellar explosion recorded by Chinese astronomers in 1054 C.E.. It is located at a distance of 2 kpc from Earth, and is energized by a powerful pulsar of spindown luminosity $L_{PSR} = 5 \cdot 10^{38}$ erg s^{-1}, and spin period $P = 33$ ms (*2*–*4*). Optical and X-ray images of the inner nebula show (*1*, *5*–*7*) features such as wisps (composing a torus-shaped structure), knots and the anvil [positioned along the South-East “jet” originating from the pulsar, and aligned with its rotation axis (*6*)]. Wisps, some of the knots, and the anvil are known to brighten and fade over weeks or months (*6*, *8*). The Crab Nebula X-ray continuum and gamma-rays up to ~100 MeV energies are modelled by synchrotron radiation, and emission from GeV to TeV energies as inverse Compton radiation by accelerated electrons scattering CMB and nebular photons (*9*–*12*).

The AGILE satellite (*13*) observed the Crab Nebula several times both in pointing mode from mid-2007/mid-2009, and in spinning mode starting in November 2009 (see Supporting Online Material, SOM). The AGILE instrument (*13*) monitors cosmic sources in the energy ranges 100 MeV – 10 GeV (hereafter, GeV gamma-rays) and 18 - 60 keV with good sensitivity and angular resolution. With the exception of a remarkable episode in October, 2007 (see below) we obtain, during standard non-active states, an average (pulsar +nebula) flux value (*14*) of $F_g = (2.2 \pm 0.1) \cdot 10^{-6}$ ph. cm^{-2} s^{-1} in the range

100 MeV - 5 GeV, for an average photon index α = 2.13 ± 0.07.

During routine monitoring in spinning mode in September, 2010, a strong and unexpected gamma-ray flare from the direction of the Crab Nebula was discovered (*15*) by AGILE above 100 MeV. The flare reached its peak during 19-21 September 2010 with a 2-day flux of $F_{g,p1}$= (7.2 ± 1.4)·10^{-6} ph cm^{-2} s^{-1} (α = 2.03 ± 0.18) for a 4.8 s.d. detection above the average flux. It subsequently decayed within 2-3 days to normal average values (Fig. 1, top panel). This flare was independently confirmed by *Fermi*-LAT (*16,17*), and different groups obtained multifrequency data in the following days (*18*). Recognizing the importance of this event was facilitated by a previous AGILE detection with similar characteristics.

AGILE detected indeed another remarkable flare from the Crab in October, 2007 [see also (*14*)]. The flare extended for ~2 weeks and showed an interesting time sub-structure (Fig. 1, bottom panel). The peak flux was reached on 7 October 2007 and the 1-day integration value was $F_{g,p2}$ =(8.9±1.1)·10^{-6} ph. cm^{-2} s^{-1} (α = 2.05 ± 0.13) for a 6.2 s.d. detection above the standard flux.

For both the October 2007 and September 2010 events there was no sign of variation of the pulsar gamma-ray signal (*19–21*) during and after these flares, as independently confirmed for the Sept.-2010 event by gamma-ray (*22*), radio (*23*), and X-ray analyses (see SOM). We thus attribute both flares to unpulsed relativistic shock emission originating in the nebula.

In the following, we focus on the September 2010 flare. Optical and X-ray imaging (*18*) shows no additional source in the Crab region during and after the flare. We note that the flaring GeV spectrum is substantially harder than the standard nebular emission (*10–12*). Fig. 2 shows the high-resolution (arcsecond) optical and X-ray images of the nebula obtained 1-2 weeks after the flare by the *Chandra* Telescope and the *Hubble Space Telescope* (HST). A few nebular brightened features are noticeable in both images. The first one is the optical and X-ray anvil feature close to the base of the pulsar jet, a primary site of shocked particle acceleration in the inner nebula (*6*, *8*). Another brightened feature is at a larger distance from the pulsar, and appears as an elongated striation in both the HST and *Chandra* images.

Important constraints can be derived from the gamma-ray flare luminosity and timescale. The peak isotropic gamma-ray luminosity $L_p \approx 5\cdot10^{35}$ erg s^{-1} implies for, e.g., a (3-5) % radiation efficiency (*24–26*), that about (2-3) % of the total spindown pulsar luminosity was dissipated at the flaring site. This large value suggests that the production region was close to the pulsar. Also the flare risetime (~1 day) favors a compact emission region of size $L \leq 10^{16}$ cm. The anvil feature is an excellent flare site candidate, also because of its alignment with the relativistic pulsar jet (*1*, *6*, *8*). This region is expected to be dominated by the leptonic current from the polar jets (*24*, *26*).

Gamma-ray flaring from the Crab Nebula provides a unique opportunity to constrain particle acceleration and radiative processes in a nebular environment. Synchrotron emission from a fresh population of shock accelerated electrons/positrons along the pulsar polar jet can explain the flaring emission in the range 0.1-10 GeV. Fig. 3 shows our flare spectral data and two examples of modelling for different assumptions on the particle populations downstream of the shock (a pure electron-positron relativistic Maxwellian distribution, and a distribution modified by a power-law component). Maxwellian and power-law models predict similar synchrotron radiation fluxes in the GeV band as shown in Fig. 3. However, if the emission from the anvil feature is related to the gamma-ray flaring, power-law models can explain also the X-ray emission from that region. Fast cooling of the highest energy particles drastically decreases the GeV flux within a few days, as observed in both the September 2010 and October 2007 flares.

These gamma-ray flares test and constrain theoretical models applicable to pure pair plasmas (*25–28*) or to distributions modified by the presence of ions that resonantly accelerate pairs by magnetosonic waves (*24*, *26*, *29*). The acceleration rate resulting from local wave absorption at the relativistic (electron or ion) cyclotron frequency and from hydrodynamical constraints is determined to be $R_{acc} \sim (\text{day})^{-1}$, implying a flare region size $L \approx 10^{16}$ cm for a standard downstream sound speed. Furthermore, reconciling the synchrotron cooling timescale $\tau \approx (8\cdot10^{8}\ \text{sec})\ B^{-2}\ \gamma^{-1}$ (where the magnetic field B is in Gauss, and γ is the particle Lorentz factor) with our observations implies, for a Lorentz factor $\gamma \approx (1\text{-}3)\cdot10^{9}$ of electrons irradiating in the GeV range, a local magnetic field $B \approx 10^{-3}$ G that is 3-10 times the nebular average (*6*, *12*). Both the 2007 and 2010 gamma-ray flares have similar spectral characteristics (Fig. 3). This observation suggests that a common acceleration process produced electron/positron energy distributions with similar physical parameters.

Considering the AGILE exposure of the Crab Nebula, we estimate that 1-2 strong gamma-ray flares actually occur per year. The Crab Nebula is thus not a standard candle at gamma-ray energies. Significant variations of the Crab Nebula high-energy flux have also been recently reported at X-ray (*30*) and TeV (*31*) energies. It remains to be established whether the gamma-ray flares that we report can be attributed to pulsar activity injecting fresh particles in the surroundings, or to major plasma wave instabilities in the nebular environment.

References and Notes

1. J. J. Hester, *Annual Rev. Astron. Astrophys*. **46**, 127 (2008).

2. M. J. Rees & J. E. Gunn, *Mon. Not. R. Astron. Soc.* **167**, 1 (1974).
3. M. Dobrowolny & A. Ferrari, *Astron. & Astrophys.* **47**, 97 (1976).
4. C. F. Kennel & F. V. Coroniti, *Astrophys. J.* **283**, 710 (1984).
5. J. D. Scargle, *Astrophys. J.* **156**, 401 (1969).
6. J. J. Hester, P. A. Scowen, R. Sankrit *et al.*, *Astrophys. J.* **448**, 240 (1995).
7. M. C. Weisskopf, J. J. Hester, A. F. Tennant, R. F. Elsnor, N. S. Schulz *et al., Astrophys. J.* **536**, L81 (2000).
8. J. J. Hester, K. Mori, D. Burrows *et al.*, *Astrophys. J.* **577**, L49 (2002).
9. O. C. de Jager, A. K. Harding, *Astrophys. J.* **396**, 161(1992).
10. O. C. de Jager *et al.*, *Astrophys. J.* **457**, 253 (1996).
11. A. M. Atoyan, F. A. Aharonian, *Mon. Not. R. Astron. Soc.* **278**, 525 (1996).
12. M. Meyer, D. Horns, H. S. Zechlin, *Astron. Astrophys*. in press, arXiv:1008.4524 (2010).
13. M. Tavani *et al.*, *Astron. Astrophys.* **502**, 995 (2009).
14. C. Pittori *et al.*, *Astron. Astrophys.* **506**, 1563 (2009).
15. M. Tavani *et al.*, *Astron. Telegram* 2855 (2010).
16. R. Buehler *et al.*, *Astron. Telegram* 2861 (2010).
17. A. A. Abdo, et al. arXiv:1011.3855v1.
18. Astronomical Telegrams nos. 2856, 2858, 2866, 2867, 2868, 2872, 2879, 2882, 2889, 2893, 2903.
19. J. M. Fierro *et al.*, *Astrophys. J.* **494**, 734 (1998).
20. A. Pellizzoni *et al.*, *Astrophys. J.* **691**, 1618 (2009).
21. A. A. Abdo *et al.*, *Astrophys. J.* **708**, 1254 (2010).
22. E. Hays *et al.*, *Astron. Telegram* 2879 (2010).
23. C. M. Espinoza *et al.*, *Astron. Telegram* 2889 (2010).
24. J. Arons, Pulsars: progress, problems and prospects, in Springer Lecture Notes. *"Neutron Stars and Pulsars, 40 years after the discovery"*, ed. W. Becker (2008).
25. G. J. Kirk, A. W. Guthmann, Y. A. Gallant, A. Achteberg, *Astrophys. J.* **542**, 235 (2000).
26. A. Spitkovsky & A. Arons, *Astrophys. J.* **603**, 669 (2004).
27. U. Keshet & E. Waxman, *Phys. Rev. Letters* **94**, 111102 (2005).
28. B. Reville & J. G. Kirk, *Astrophys. J.* in press, arXiv:1010.0872v1 (2010).
29. Y. A. Gallant & J. Arons, *Astrophys. J.* **435**, 230 (1994).
30. C.A. Wilson-Hodge, et al., arXiv:1010.2679v1 [astro-ph.HE] (2010).
31. G. Aielli, *et al., Astron. Telegram* 2921 (2010).

32. We thank the *Chandra* Observatory Director H. Tananbaum, the *Hubble Space Telescope* Director M. Mountain, N. Gehrels and the *Swift* team for their prompt response in carrying out the observations reported in this paper. Research partially supported by the ASI grant no. I/089/06/2.

Supporting Online Material
www.sciencemag.org/cgi/content/full/science.1200083/DC1
SOM Text
Figs. S1 to S5
Table S1
References

21 October 2010; accepted 13 December 2010
Published online 6 January 2011; 10.1126/science.1200083

Fig. 1. Crab Nebula lightcurves of the total flux detected by AGILE in the energy range 100 MeV – 5 GeV during the gamma-ray flaring periods in 2007 and 2010 (units of 10^{-8} ph cm^{-2} s^{-1}). *(Top panel:)* the "spinning" AGILE photon flux lightcurve during the period Sept. 2 - Oct. 8, 2010. Time bins are 2.5 days except near the flare peak (2-day binning). Errors are 1 s.d. and time is given in Modified Julian Day (MJD). The dotted line and band marked in grey color show the average Crab flux and the 3 s.d. uncertainty range. *(Bottom panel:)* The AGILE lightcurve during the period Sept. 27 – Oct. 12, 2007 (1-day binning) with the satellite in pointing mode. Errors are 1 s.d. Time is given in Modified Julian Day (MJD). The dotted line and band marked in grey color show the average Crab flux and the 3 s.d. uncertainty range.

Fig. 2. HST and Chandra imaging of the Crab Nebula following the Sept., 2010 gamma-ray flare. *(Top left panel:)* optical image of the inner nebula region (approximately 28"x28", North is up, East on the left) obtained by the ACS instrument on board the *Hubble Space Telescope* (HST) on October 2, 2010. ACS bandpass: 3,500-11,000 Angstrom. The pulsar position is marked with a green arrow in all panels. White arrows in all panels mark interesting features compared to archival data. *(Top right panel:)* the same region imaged by the *Chandra* Observatory ACIS instrument on September 28, 2010 in the energy range 0.5-8 keV (level-1 data). The pulsar does not show in this map and below because of pileup. *(Bottom left panel:)* zoom of the HST image (approximately 9"x9"), showing the nebular inner region, and the details of the "anvil feature" showing a "ring"-like structure at the base of the South-East "jet" off the pulsar. "Knot 1" at 0".6 South-East from the pulsar is saturated at the pulsar position. Terminology is from ref. *6*. *(Bottom right panel:)* zoom of the *Chandra* image, showing the X-ray brightening of the "anvil" region and the correspondence with the optical image. Analysis of the features marked "A", "B", and "C" gives the following results in the energy range 0.5-8 keV for the flux F, spectral index α, and absorption N_H (quoted errors are statistical at the 68% c.l.). Feature A: flux $F = (48.5 \pm 8.7) \cdot 10^{-12}$ erg cm^{-2} s^{-1}, α

$=1.76 \pm 0.30$, $N_H = (0.36 \pm 0.05) \cdot 10^{22}$ atoms cm^{-2}. Feature B: flux $F = (26.6 \pm 5.9) \cdot 10^{-12}$ erg cm^{-2} s^{-1}, $\alpha = 1.76 \pm 0.41$, $N_H = (0.34 \pm 0.05) \cdot 10^{22}$ atoms cm^{-2}. Feature C: flux $F = (25.3 \pm 5.9) \cdot 10^{-12}$ erg cm^{-2} s^{-1}, $\alpha = 1.46 \pm 0.36$, $N_H = (0.34 \pm 0.04) \cdot 10^{22}$ atoms cm^{-2}.

Fig. 3. Spectral energy distribution of the Crab Nebula and the flaring gamma-ray episodes (the pulsar signal has been subtracted). Open black symbols: Crab Nebula emission in the steady state. The dashed curve shows our modelling of the steady state [see also (*1*, *21*, *12*)]. The solid black curve shows our flare modelling for energies above 10^5 eV. Dotted black curve: nebular IR emission (*1*). (*Top panel:*) blue filled symbols: spectral AGILE gamma-ray flare data integrated over 2 days (September 19-21, 2010, MJD 55458.5-55460.5). Errors are 1 s.d. Solid red and blue curves show the 2-day averaged spectral models based on synchrotron radiation from relativistic electrons/positrons impulsively accelerated in a shock region of size $L \leq 10^{16}$ cm . Dotted curves show the spectra evolved by synchrotron cooling 3 days after the flare. The blue curve model is based on a relativistic Maxwellian distribution of critical energy (Lorentz factor) $\gamma^* = 10^9$ (for a local $B = 10^{-3}$ G) representing the differential energy distribution of accelerated electrons. The red curve model is characterized (for a local $B = 10^{-3}$ G) by a double power-law electron differential distribution $dN(\gamma)/d\gamma = \gamma^{-p1}$ for $\gamma_{\rm min} < \gamma < \gamma_{\rm break}$ with $p_1 = 2.1$, $\gamma_{\rm min} = 5 \cdot 10^5$, $\gamma_{\rm break} = 10^9$, and $dN(\gamma)/d\gamma = \gamma^{-p2}$ for $\gamma_{\rm break} < \gamma < \gamma_{\rm max}$, with $p_2 = 2.7$, $\gamma_{\rm max} = 7 \cdot 10^9$, and a total particle number $N_{e-/e+} = 10^{42}$. This model is extended towards the low-energy range, and can account for the local X-ray spectral enhancements in the "anvil" region as observed by *Chandra* (see Fig. 2). The area marked in green represents the 1 s.d. X-ray spectral data for feature "A" of Fig. 2. (*Bottom panel:*) violet symbols: spectral AGILE gamma-ray data during the October 7-9, 2007 flare (MJD 54380.5-54382.5). Errors are 1 s.d. The black, blue and red curves are those of the Sept. 2010 flare, and are shown here as a reference to compare the two spectra.

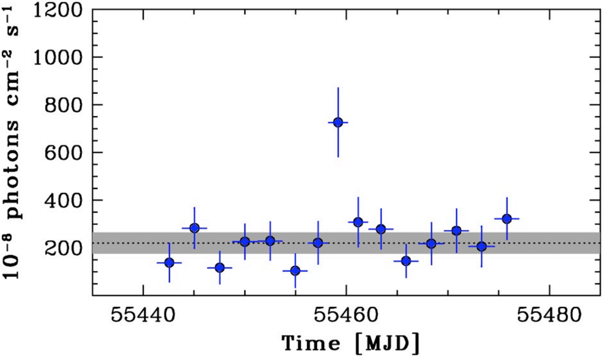
10^{-8} photons cm^{-2} s^{-1}
1200
1000
800
600
400
200
55440
55460
55480
Time [MJD]

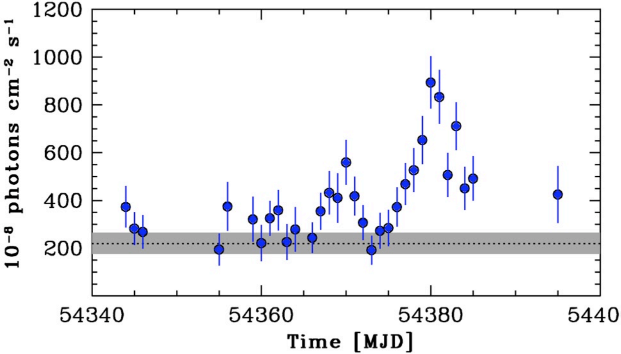
10^{-8} photons cm^{-2} s^{-1}
1200
1000
800
600
400
200
54340
54360
54380
54400
Time [MJD]

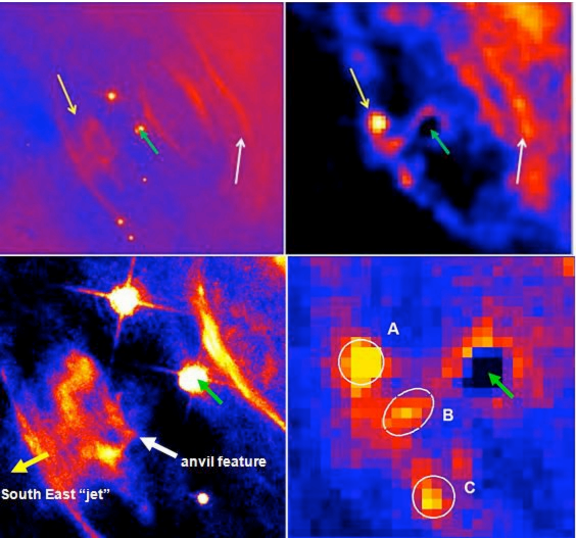
A
B
C
anvil feature
South East "jet"

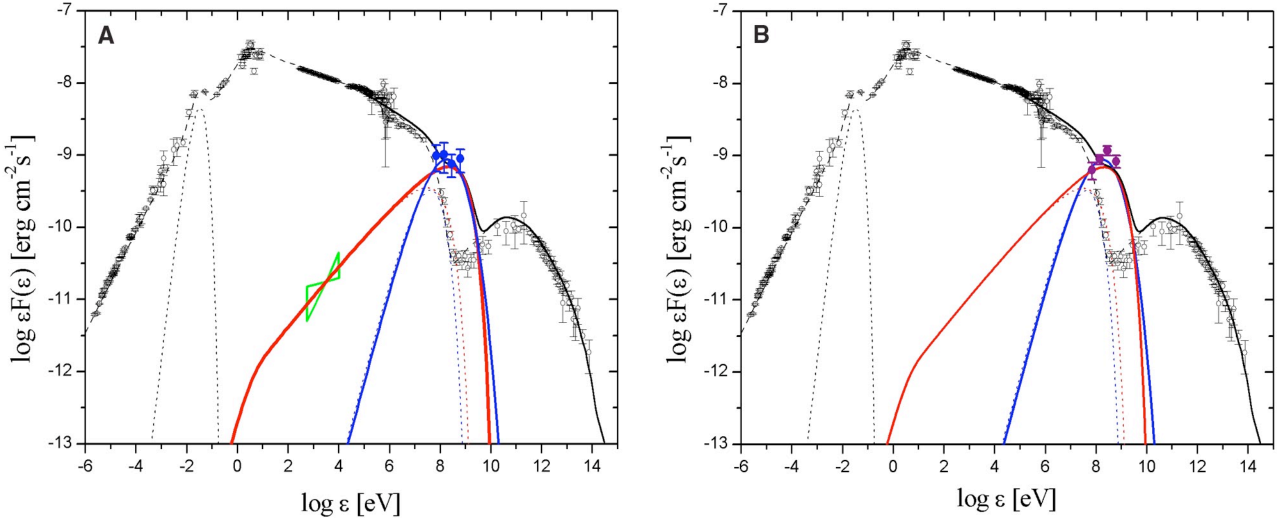
A
B
log εF(ε) [erg cm^{-2}s^{-1}]
-7
-8
-9
-10
-11
-12
-13
-6
-4
-2
0
2
4
6
8
10
12
14
log ε [eV]